15th Australasian Fluid Mechanics Conference
The University of Sydney, Sydney, Australia
13-17 December 2004

Free Surface Monitoring Using Image Processing

P.D.M. Brady[1], M. Boutounet[2] and S. Beecham[1]

[1] Faculty of Engineering
University of Technology Sydney, NSW, 2007 AUSTRALIA

[2] Département de Génie Mathématique et Modélisation
INSA Toulouse, 31077 Toulouse Cedex 4, FRANCE

Abstract

We present an alternate method of data capture based on a consumer grade digital video camera combined with commonly available image processing techniques. The capture/analysis technique was developed to provide experimental data for the validation of free surface Computational Fluid Dynamics (CFD) models and records the wave motion along the inside of the flume walls. A sample data set is presented as validation of the capture/analysis technique.

ntroduction

The validation of free surface Computational Fluid Dynamics models requires more data than can be supplied by Laser Doppler Velocimetry (LDV), Constant Temperature Anemometry (CTA) or Particle Image Velocimetry (PIV) alone. LDV, CTA and PIV are very expensive to both set up and run and as a result access is restricted to those institutions that have the resources to purchase and maintain these types of sensors. They also require a high level of expertise to operate and only provide data on the structure of the velocity field. Additional validation data can be obtained by measurement of the free surface using manual or automatic point probes although these approaches also have their limitations.

Figure 1 shows an image of free surface CFD data that requires validation. The flow is representative of water draining out of a flume around a square cylinder that is piercing the free surface. The free surface is shown within the wire frame walls and is coloured by the velocity magnitude of the particles in the vicinity.

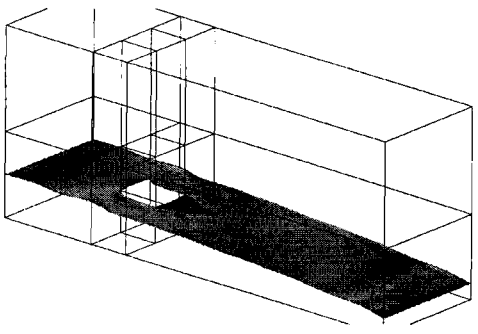

Figure 1: Example CFD data with waves along the walls, only the free surface is shown which has been coloured by speed. The flow is from left to right

Alternatively the use of a consumer grade digital video camera and off the shelf image processing software can provide detailed information on the wave motion, which in turn provides direct, quantitative validation data for CFD validation studies.

The increase of image quality of consumer grade digital cameras means that they can directly compete with commercial PIV systems in terms of pixel resolution. The system discussed in this paper has several advantages over PIV: the lack of flow seeding and seed resolution. There are experimental configurations where it is impractical, if not impossible, to adequately seed the flow for the use of PIV techniques such as a recirculating flume where the particles may damage the pump or other devices. As the technique presented here does not use seed particles it will be suitable in these situations. A further limitation of PIV systems that they are based on mathematical correlations of seed particles, which generally require a window of at least 5x5 pixels for correlation. However, the optical technique presented in this paper is limited by the resolution of the camera used rather than the pixel window of the correlation function.

The image processing described in this paper was undertaken using MATLAB™ [2] and the MATLAB Image Processing Toolbox™ because they are available within the Faculty of Engineering, UTS. However all the methods described below could be implemented on alternative software packages.

Hardware Configuration and Data Capture

The experimental testing was undertaken using the 13m tilting open channel flume located in the Hydraulics Laboratory at the Faculty of Engineering, UTS. The flume is 305mm wide by 305mm deep, has a smooth opaque floor and transparent glass walls. An inlet diffuser is installed to evenly distribute the flow from the incoming pipe, while an adjustable overflow weir provides outlet control. Feed water is provided by a recirculating ring main system that is supplied by a Worthington 52R-13A type pump fed from a return sump.

The image capture process was undertaken using a Sony miniDV camcorder, model DCR-PC110E, which was connected to a computer via an IEEE 1394b (Firewire) interface. Two methods of data capture were tested: direct computer capture and recording to a miniDV tape.

The computer used for the data capture was a Macintosh G4 Powerbook running MACOS™ 10. Analysis of the images was undertaken on the Faculty of Engineering Research Computing Cluster using MATLAB™ release 6.5 in a Linux environment. The Linux cluster is a collection of workstations dedicated to high speed computing based on Pentium 4 3GHz processors with an 800MHz front side bus and 2Gb of 400MHz DDR-RAM.

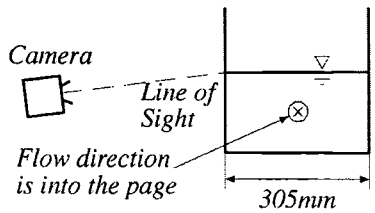

Figure 2: Schematic of the camera location relative to the flume

The focal plane of the camera was set up slightly under the flume so that the camera was looking up to the free surface. This is necessary so that the analysis, which is based on an image detection routine, detects the free surface on the wall and not a wave moving through the centre of the channel. The camera was set back approximately 1m from the walls as shown in Figure 2. Several methods of illuminating the flume were tested and included:

- Room fluorescent lighting only,
- Room fluorescent lighting augmented with a 200W floodlight,
- Floodlight only.

In this case the optimal lighting configuration was the floodlight only. We infer that this was because we had direct control of the direction and intensity of the light. The floodlight would have also eliminated stray light sources from the rest of the laboratory that might have introduced additional shadowing. We suspect that the lighting may need to be tailored for each experimental application.

A 50mm grid was attached to the side of the flume to be filmed. An image of the grid was then taken and used to transform the image to eliminate the curvature introduced as a result of the camera lens.

Data Analysis

Image Rectification

The first step in reducing the raw video data as recorded by the camera was to coordinate and rectify the base image. This allows the free surface as captured by the edge detection methods to be expressed in real world coordinates rather than a pixel-based coordinate scheme.

To begin the transformation a selection of control points are graphically selected as shown in Figure 3. The interface allowed the user to simply click at the selected grid intersections.

Figure 3: Image registration grid

These points were then assigned their real cartesian coordinates for the transformation. The transformation was based on the discrete linear transform (DLT) method presented by Abdel-Aziz and Karara [1]. A set of control points, entered by the user, were used to define eight parameters, which is the minimum required for a two-dimensional problem. At least four pairs of points are required to compute the transform which was based on a least squares method. A discussion of the accuracy of this method is presented below. A colour image of the transformed grid is shown in Figure 4.

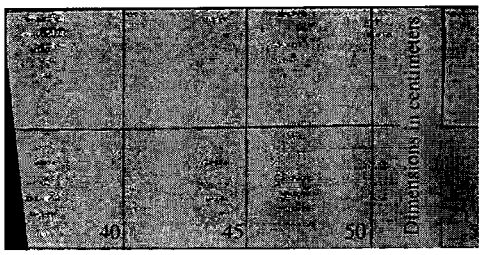

Figure 4: Rectified image of the grid

The next step in analysing the data was to reduce the number of colours in the data from Red/Green/Blue (RGB) to black and white (BW). Four BW reductions were tested: the combined RGB image and the three individual colour channels. Computationally there is little difference in processing overheads from working with the combined or individual channel data. The single green channel, when reduced to black and white, produced the cleanest BW edge. Figure 5 shows the black and white reduction of the green channel data.

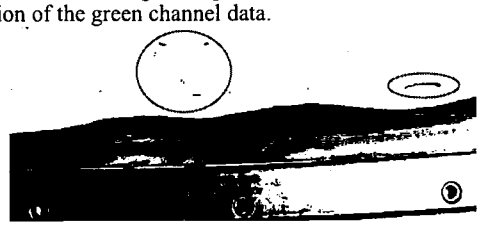

Figure 5: Black and white reduction of the green channel data, note the metallic base of the flume with bolts along the bottom of the image. The ellipsoid indicators show where marks on the flume need to be masked. The flow is moving from left to right in this image

Once the image had been reduced to black and white a mask was applied to hide the areas that are not of interest or that contained potentially spurious data. For example there are several marks shown on Figure 5 that are on the flume walls and are not part of the required data set. This mask, like the transform function, was applied to the whole data set and therefore it had to be carefully selected so that the free surface did not infringe on the masked area during the transient data series.

Edge Detection

The black and white image is stored as a logical array with the black and white pixels represented by FALSE (0 or off) and TRUE (1 or on) respectively. Using the logical array allows the edge detection to be based on the location of the change from FALSE to TRUE.

The edge detected by the edge detection routine is saved in a n x *nframes* array where the n dimension represents the number of pixels in the image and *nframes* is the number of still images that have been analysed. Usually the maximum frame rate for consumer digital video cameras is 25Hz and 29.97Hz for PAL and NTSC respectively. The value stored in the array at location n_i is the height of the free surface in pixels. Figure 6 shows a typical view of the free surface data as it is extracted from the edge detection routine and before any transforms are applied.

Spurious data points may be introduced as a result of the logical array at the boundaries. This is shown in Figure 6 for the highest time frame and between the 400 and 600 points on the x pixel axis. An interpolation function, combined with boundary filtering can be implemented at this stage to eliminate these data points. See the sample data section for a detailed discussion and example of these errors.

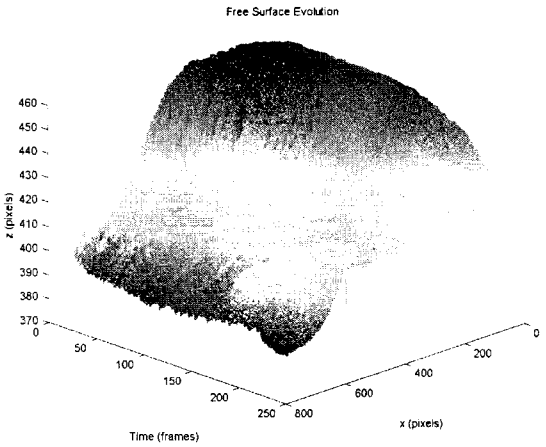

Figure 6: The raw processed data after extraction of the free surface and before applying the transforms to real time and space.

\ transformation, which is based on the original coordination points, is then used to translate the measured coordinates from pixel space to physical space. These transformed coordinates are then based in the coordinate system used for the rectification step.

Sample Data

Experimental Configuration

Sample data for validating the software were collected for a hydraulic jump moving upstream as shown in Figure 7. The upstream flow rate was set to 4l/s and the flume was set at a 1/250 slope. Supercritical flow was generated using an adjustable sluice gate set at a 20mm opening while the downstream control was provided by an adjustable weir.

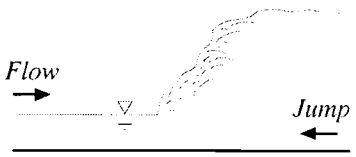

Figure 7: Sketch of the relative motion of the hydraulic jump and flow

Initially the downstream control was relaxed so that the flow remained supercritical for the entire length of the flume downstream of the sluice. Once the flow had been established the weir was lifted to approximately three times the height of the critical depth. This backpressure caused the formation of a hydraulic jump, which then moved upstream and through the data capture window.

Analysis

The data captured was reduced to black and white and the edge detected as outlined above. A plot of this raw data is shown in Figure 8, which clearly shows the boundary errors introduced at the left and right edges of the frame. Stray pixel data, visible as vertical lines extending a large distance below the surrounding points, are also visible at around the 450 pixel mark on the distance axis, occurring over intermittent time steps.

Stray pixels can be removed from the data set via an interpolation scheme based on the adjacent data. This method is discussed below in the *Image Errors* section.

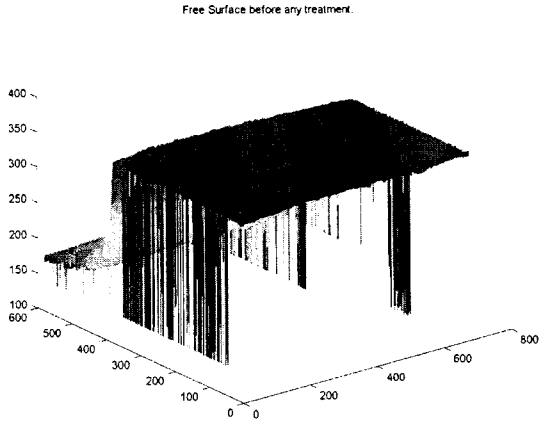

Figure 8: Raw pixel data with the vertical, left and right axes representative of image height (pixels), frame number and distance (pixels) respectively

The edge filtering allows for the removal of a fixed number of data points from either side. This filtering process is subjective and must be undertaken by the operator to ensure that spurious data are removed only. Figure 9 shows the results of the transformed and smoothed data.

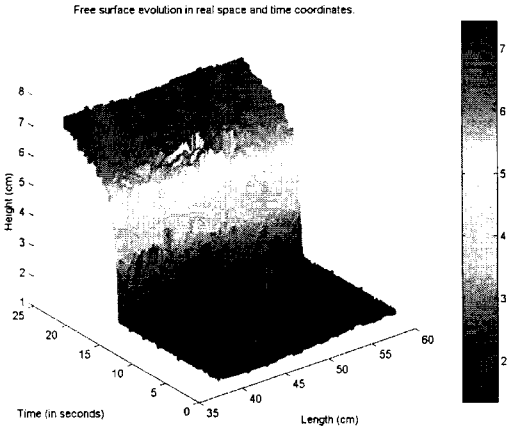

Figure 9: Transformed and filtered data, coloured by depth in centimetres

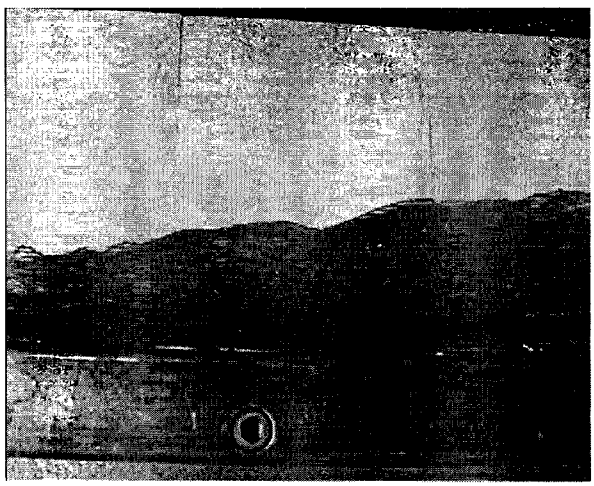

Figure 10: Image of the free surface superimposed over the original data

Figure 10 shows an inspection image of the free surface data superimposed over the original image data. This allows for a quick visual inspection to test the accuracy of the analysis.

Potential Numerical Inaccuracies

It should be stressed that this method is not as accurate as single point probe techniques. However the strength of the method is that it provides data across the entire field of view. This gives the potential to capture the entire shape of the wave as opposed to measuring the wave passage only. Some of the factors that will affect the accuracy of the procedure are discussed below.

Rectification

The discrete linear transform used to rectify the images directly calculates an estimate of the numerical error using the mean of the Euclidean norms of vectors,

$$x_{real}(i) - transformed\left(x_{pixels}(i)\right), 1 \le i \le n_p, \qquad (1)$$

where n_p is the number of coordination points used. For example the grid shown in Figure 3, which was approximately 200x100mm, when transformed with a four point transform had an estimated error of 3.66mm and an error of 2.95mm for ten points. This equates to a 20% reduction in the estimated error.

A test was undertaken with a larger field of view, in this case a 350x200mm grid. For a four and six point transformation the estimated error came to 4.16 and 4.9mm respectively. Examination of this result showed that at larger grids the user selection becomes dominant in the error magnitude rather than the transformation process.

It may be possible to reduce the error introduced by the user selection process by converting the hollow grid currently used to that of a filled checkerboard grid. This would allow the use of a corner detection routine with the user entering the appropriate coordinates for the points found by the routine. Investigation of this method will be a topic for future research.

Parallax Error

A parallax error will be introduced as the light rays pass at an oblique angle through the glass of the flume. Given an approximate refractive index of glass, relative to air, of n=1.50 and the maximum angle of incidence (θ_i) of 45° (based on a focal length of 42mm at the widest angle [3], θ_r is the angle of refraction) the maximum offset (o) would be 4.2mm based on the 5mm (t) thickness of glass installed in the flume, see Figure 11. The parallax error would be reduced when using the camera at higher focal lengths or when it is located closer to the flume.

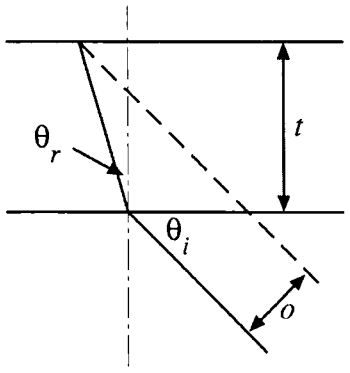

Figure 11: Parallax error

Care must be taken when choosing both the camera type and it's location for the experiment to ensure the pixel error is appropriate. The maximum accuracy of the free surface detection is to the pixel that it is in. As an example using a 640x480 video pixel camera, which is common for consumer video cameras, and shooting a 20cm by 10cm window for width and depth respectively yields an approximate pixel size of 0.3mm. These dimensions correspond roughly to the data illustrated above in the sample section and this accuracy is an order of magnitude less than the errors introduced by parallax or the meniscus however they may become a problem for larger applications or when a macro lens is used.

Image Errors

Stray pixel data can accumulate as shown in Figure 8 and can be removed using an interpolation scheme. The interpolation scheme used here was based on linear interpolation between the adjacent points that were considered real.

As the user has little control over the implementation of this interpolation scheme care must be taken when examining the final data for inaccuracies.

Computational Requirements

The sample data processed took an average of 0.7s per frame for analysis. This time is inclusive of image rectification and converting back to an animation.

In order to eliminate the need for the user to be at the program, the software has been configured to run in either a graphical or batch mode. Thus this run time can be undertaken overnight using the batch settings.

Alternate Implementation Schemes

An alternate capture technique aimed to provide validation data of the flow field around the square cylinder, shown in Figure 1, is being developed. The technique uses a transparent cylinder mounted in the flume and has a fixed mirror in the centre of the cylinder. The camera would then be mounted above the cylinder so that the free surface image is reflected via the mirror to the camera for capture. This technique is currently under development with details to be published upon completion of the development.

Conclusions

We have presented an alternative data capture and analysis technique based on a consumer quality digital video camera and readily available image processing software. Possible applications of the technique include providing validation data for free surface CFD models and experimental wave analysis. A sample data set has been presented for validation of the method, which shows that the method is applicable within the constraints outlined.

A limitation of the system was identified in that the capture is based on the boundary of the flow rather than the middle of the flow domain. This indicates that the method does provide useful information but is not a complete analysis system in itself and should be used in conjunction with other methods such as PIV or LDV.

Acknowledgments

This work would not have been possible without the collaborative relationship between Institut National des Sciences Appliquées (INSA), Toulouse and the Faculty of Engineering, UTS. The MATLAB Image Processing Toolbox was made available within the Faculty of Engineering, UTS by Professor Hung Nguyen.

References

[1] Abdel-Aziz, Y. I. and Karara, H. M., Direct Linear Transform From Comparator Coordinates Into Object Space Coordinates in Close-Range Photogrammetry, presented in *Symposium on Close Range Photogrammetry*, Falls Church, Virginia, USA, 1971.

[2] Mathworks, MATLAB 6.5, 6.5.0.180913a Release 13 ed. Natick, Massachusetts, USA: The Mathworks Incorporated, 2002.

[3] Sony, *Sony Digital Video Camera Recorder - Model DCR-PC110*. Park Ridge, New Jersey, USA: Sony, 2000.

Proceedings of the Fifteenth Australasian Fluid Mechanics Conference

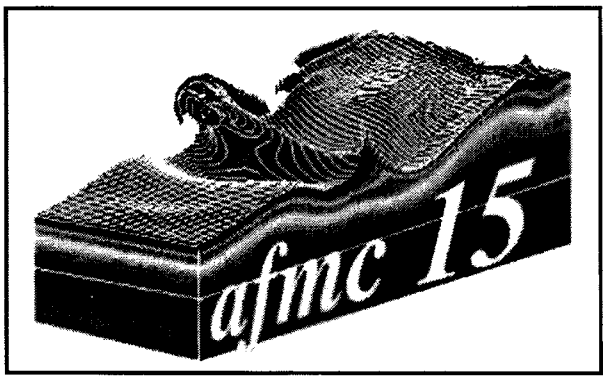

13–17 December 2004, The University of Sydney

edited by M. Behnia, W. Lin, & G. D. McBain

Publisher: The University of Sydney, Sydney NSW 2006 Australia, tel. +61-2-9036 9518, fax +61-2-9036 9519, e-mail *15afmc@aeromech.usyd.edu.au*

ISBN: 1-864-87695-6 (CD-ROM)

All papers in these proceedings have been reviewed by an independent panel of experts.

Responsibility for the contents of the papers rests solely upon the authors.

Example of how one of these papers might be cited:

Antonia, R. A., and Burattini, P., Small-scale turbulence: how universal is it?, in *Proceedings of the Fifteenth Australasian Fluid Mechanics Conference (CD-ROM),* editors M. Behnia, W. Lin, and G.